PUPT-1905 IASSNS-HEP-99-112 hep-th/9912072

arXiv:hep-th/9912072v2 21 Dec 1999

Noncommutative Perturbative Dynamics

Shiraz Minwalla, Mark Van Raamsdonk[1],

Department of Physics, Princeton University
Princeton, NJ 08544, USA

and

Nathan Seiberg[2]

School of Natural Sciences, Institute for Advanced Study
Olden Lane, Princeton, NJ 08540, USA

Abstract

We study the perturbative dynamics of noncommutative field theories on $\mathcal{R}^d$, and find an intriguing mixing of the UV and the IR. High energies of virtual particles in loops produce non-analyticity at low momentum. Consequently, the low energy effective action is singular at zero momentum even when the original noncommutative field theory is massive. Some of the nonplanar diagrams of these theories are divergent, but we interpret these divergences as IR divergences and deal with them accordingly. We explain how this UV/IR mixing arises from the underlying noncommutativity. This phenomenon is reminiscent of the channel duality of the double twist diagram in open string theory.

Dec. 1999

[1] minwalla, mav@princeton.edu

[2] seiberg@sns.ias.edu

1. Introduction

In this note we follow [1-12] and analyze quantum field theory on a noncommutative space. For simplicity we focus on the case of the noncommutative $\mathcal{R}^d$ and in most of the note we discuss only scalar field theories (we will briefly mention gauge theories in the last section). Although noncommutative gauge theories appear in string theory [13] (see [14] and references therein for recent developments), through most of the paper our discussion will be field theoretic.

The underlying $\mathcal{R}^d$ is labeled by d noncommuting coordinates satisfying

$$[x^\mu, x^\nu] = i\Theta^{\mu\nu}. \tag{1.1}$$

Here $\Theta^{\mu\nu}$ is real and antisymmetric. By a choice of coordinates Θ can be brought to the form

$$\begin{pmatrix} 0 & \theta_1 & & \\ -\theta_1 & 0 & & \\ & & \ddots & \end{pmatrix}. \tag{1.2}$$

Thus a Θ matrix of rank r describes a spacetime with $\frac{r}{2}$ pairs of noncommuting coordinates and $d-r$ coordinates that commute with all others.

The algebra of functions on noncommutative $\mathcal{R}^d$ can be viewed as an algebra of ordinary functions on the usual $\mathcal{R}^d$ with the product deformed to the noncommutative, associative star product, defined by

$$\big(\phi_1 \star \phi_2\big)(x) = e^{\frac{i}{2}\Theta^{\mu\nu}\partial^y_\mu \partial^z_\nu}\phi_1(y)\phi_2(z)|_{y=z=x}\ . \tag{1.3}$$

Thus, we will study theories whose fields are functions on ordinary $\mathcal{R}^d$, with actions of the usual form $S = \int d^dx\mathcal{L}[\phi]$, except that the fields in $\mathcal{L}$ are multiplied using the star product.

In section 2 we take a first look at the perturbation theory of noncommutative scalar field theories. After deriving the Feynman rules, we review the results of Filk [1], who showed that planar diagrams in noncommutative field theories are essentially the same as those in the corresponding commutative theory.

Section 3 is devoted to a detailed analysis of one loop diagrams and especially to nonplanar one loop diagrams in ϕ^3 in six dimensions and ϕ^4 in four dimensions. These diagrams are UV finite but exhibit interesting IR singularities. In particular, even though the theory we start with is massive, its correlation functions exhibit singularities at zero momenta!

This nontrivial mixture between UV and IR phenomena is perhaps the most surprising result of this paper. It is tempting to speculate that such mixing of scales could be relevant to various hierarchy problems like the problem of the cosmological constant.

In section 4 we point out that the IR singularities of section 3 are quite similar to the appearance of closed string poles in the double twist diagram in open string theory. It is surprising that a field theory exhibits such a stringy phenomenon.

In section 5 we explore higher order Feynman diagrams and some of their properties. We also consider the limit of maximal noncommutativity, $\Theta \to \infty$. In this limit the theory is dominated by planar graphs and appears to be stringy.

In section 6 we explain how the noncommutativity of spacetime leads to the surprising IR phenomena discussed in earlier sections. Section 7 is the beginning of an investigation into the properties of noncommutative gauge theories. In an appendix we present the expression for the Feynman integral corresponding to an arbitrary graph in a noncommutative theory, written in terms of Schwinger parameters.

2. First Look at Perturbation Theory

2.1. Feynman Rules

For any noncommutative theory, the quadratic part of the action is the same as in the commutative theory, since

$$\begin{aligned} \int d^d x \phi \star \phi &= \int d^d x \phi \phi \\ \int d^d x \partial\phi \star \partial\phi &= \int d^d x \partial\phi \partial\phi \end{aligned} \tag{2.1}$$

(we have dropped total derivatives assuming suitable boundary conditions on ϕ). Therefore propagators take their usual form, as in commutative theories.

The interactions are modified. We consider a polynomial interaction (perhaps with derivatives)

$$\sum_{n=3}^{L} a_n g^{n-2} \phi^n, \tag{2.2}$$

where the powers of the coupling constant g are introduced for convenience, the coefficients a_n are arbitrary numbers, and the products of ϕ are star products. In momentum space

the interaction vertex of ϕ^n has an additional phase factor relative to the commutative theory

$$V(k_1, k_2..., k_n) = e^{-\frac{i}{2}\sum_{i<j} k_i \times k_j,} \tag{2.3}$$

where k_i is the momentum flowing into the vertex through the ith ϕ and

$$k_i \times k_j \equiv k_{i\mu}\Theta^{\mu\nu}k_{j\nu}. \tag{2.4}$$

This is the only modification to the Feynman rules.

V is not invariant under arbitrary permutations of k_i and so one must keep track of the order in which lines emanate from vertices in a Feynman diagram. (Using momentum conservation, it is easy to see that $V(k_1, \cdots, k_n)$ is invariant under cyclic permutations of k_i.) One way to keep track of the order of the lines is to view ϕ as an $N \times N$ matrix and to use double line notation in the Feynman diagrams. In the noncommutative theory this is useful even when $N = 1$. Contractions which yield distinct diagrams in double line notation are associated with different contributions from the noncommutative phases.

One may associate a genus with every diagram. Specifically, the genus of a diagram is the minimum genus of a surface upon which the diagram may be drawn without any intersections. In the large N expansion, graphs are organized according to their genus. We will find it convenient to use the same organization even for $N = 1$. In the next subsection we will study the genus zero, planar diagrams.

2.2. Planar Graphs

In a planar graph it is always possible to regard momentum as an additional index flowing along the double lines. That is, given an L loop planar graph, the momenta of all lines in the graph may be written in terms of 'momenta' $l_1, \cdots, l_{L+1}$ that flow unchanged along an index line (see Fig. 1) of the graph. Like fundamental $U(N)$ matrix indices, the index line momenta along adjacent edges of a given propagator flow in opposite directions. Therefore, the momentum through any propagator (or external line) in the graph is given by $l_i - l_j$, where l_i and l_j are the index line momenta that flow along the adjacent edges of the propagator. Since index line momenta are always conserved, this construction automatically implements momentum conservation at vertices. Note that such a construction is not possible in nonplanar graphs.

For any vertex of the graph, let the momenta entering the vertex through the n propagators be $k_1, k_2, \cdots, k_n$, in cyclic order. Then $k_1 = l_{i_1} - l_{i_2}$, $k_2 = l_{i_2} - l_{i_3}, \cdots, k_n =$

$l_{i_n} - l_{i_1}$, in terms of which $(\sum_{i<j} k_i \times k_j) = l_{i_1} \times l_{i_2} + l_{i_2} \times l_{i_3} + \cdots + l_{i_n} \times l_{i_1}$. Thus the phase factor at any interaction point may be expressed as the product of n terms, one for each incoming propagator,

$$V = \prod_{j=1}^{n} e^{-\frac{i}{2}(l_{i_j} \times l_{i_{j+1}})}. \tag{2.5}$$

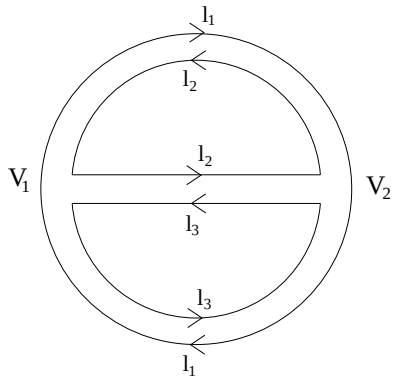

Fig. 1: A planar graph in double line notation. The phase associated with, say, the middle propagator is $l_2 \times l_3$ from the vertex V_1 and -$l_2 \times l_3$ from the vertex V_2, adding to zero.

We see that the phase associated with any internal propagator is equal and opposite at its two end vertices, and so cancels. We conclude that the phase factor associated with the planar diagram is

$$V(p_1, p_2 ..., p_n) = e^{-\frac{i}{2}\sum_{i<j} p_i \times p_j}, \tag{2.6}$$

where the sum is taken over all external momenta (in the original variables) in the correct cyclic order. This result is originally due to [1] and this derivation follows [10]. We note that this phase factor is exactly the one found in [14] by computing disk amplitudes in string theory.

It is important that this phase factor is independent of the details of the internal structure of the graph. Thus, the contribution of a planar graph to the noncommutative effective action is precisely the contribution of the same graph in the $\Theta = 0$ theory multiplied by $V(p_1, p_2, ..., p_n)$. Such a Θ dependent phase factor is present in all interaction terms in the bare Lagrangian and in all tree graphs computed either with the bare Lagrangian or with the effective Lagrangian computed with planar graphs.

At $\Theta = 0$, divergent terms in the effective action are products of local fields. $V(p_1, p_2, ..., p_n)$ modifies these to the star product of local fields. Divergences (due to

planar graphs) in the effective action at $\Theta \neq 0$ may therefore be absorbed into redefinitions of bare parameters, if and only if the $\Theta = 0$ theory is renormalizable.

We stress that this renormalization procedure is not obtained by adding local counterterms. The added counterterms are of the same form as the original terms in the Lagrangian but they are not local.

2.3. Nonplanar Graphs

Nonplanar diagrams have propagators that cross over each other, or over external lines as in Fig 2.

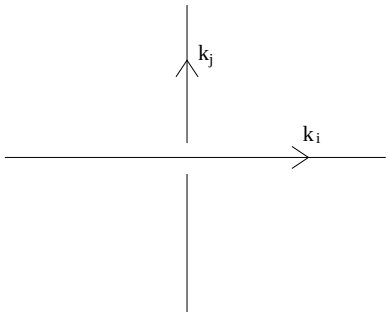

Fig. 2: Two lines crossing in a nonplanar graph.

If, instead of crossing, the two lines in Fig. 2 had met at a (4 point) vertex, the graph would have had an additional phase factor of $e^{-\frac{i}{2}(k_j \times k_i - k_j \times k_i - k_i \times k_j + k_j \times k_i)} = e^{-ik_j \times k_i}$ but would then have been planar (as far as this crossing was concerned). Therefore, any nonplanar graph will have an extra phase

$$e^{+ik_j \times k_i} \tag{2.7}$$

for each crossing of momenta k_i and k_j in addition to the phase associated with the ordering of external momenta. The complete phase for a general graph may be written [1]

$$V(p_1, p_2, ..., p_n)\; e^{-i\left(\frac{1}{2}\sum_{i,j} C_{ij} k_i \times k_j\right)}, \tag{2.8}$$

where V is as in (2.6), and C_{ij}, the intersection matrix, counts the number of times the i^{th} (internal or external) line crosses over the j^{th} line. Crossings are counted as positive if k_i crosses k_j with k_j moving to the left.

The matrix C_{ij} corresponding to a given graph is not unique, since different ways of drawing the graph will lead to different intersections (see Fig. 3). However, all of

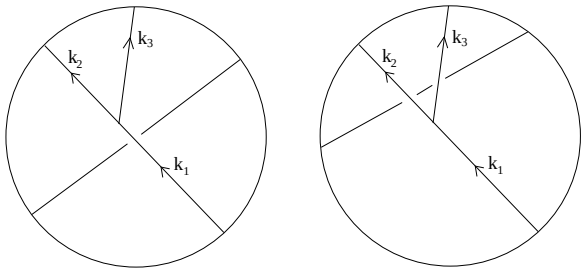

Fig. 3: The overlaps in a nonplanar Feynman diagram can be chosen in several different ways.

these yield identical Feynman integrands; the ambiguity corresponds to the fact that the internal momenta k_i of the graph are not all independent but are constrained by momentum conservation at each vertex.

As the Θ dependence of nonplanar graphs does not factor out of the integral, nonplanar graphs at $\Theta \neq 0$ behave very differently from their $\Theta = 0$ counterparts. For instance, as we will see in section 3, all nonplanar one loop diagrams are finite. The improved convergence of nonplanar graphs is a result of the damping effects of rapid oscillations of internal momentum dependent phase factors in the integrand. Since each nonplanarity in a Feynman diagram results in a new internal momentum dependent phase factor in the Feynman integrand, one is tempted to guess that every nonplanar graph is convergent. More precisely, one might conjecture that, with the exception of divergent planar subgraphs, there are no new divergences associated with nonplanar graphs. This would imply that, after the planar graphs have been renormalized, no further renormalization is needed.

In fact, it turns out that nonplanar graphs (with no divergent planar subgraphs) are not all finite in theories with quadratic or higher divergences (including all scalar theories), as we will see in section 5. This would appear to threaten renormalizability of these theories, since the nonplanar counterterms that cancelled these divergences would be complicated functions of Θ and external momenta, and have a very nonlocal and complicated form in position space. At higher orders such counterterms would generate new divergences of increasingly complicated form. It seems unlikely that this process would terminate with a finite number of terms written in terms of star products. However, we will interpret these divergences as IR rather than UV divergences and will suggest a procedure to deal with them without introducing counterterms.

3. One loop in scalar field theory

In this section we explicitly compute several one loop nonplanar graphs in ϕ^4 theory in four dimensions and ϕ^3 theory in six dimensions. We find that one loop nonplanar graphs in noncommutative field theories are convergent at generic values of external momenta. This is a consequence of the rapid oscillations of the phase factor $e^{ip\times k}$ where p is an external momentum and k is the loop momentum. As this phase factor is zero when $p_\mu\Theta^{\mu\nu}$ vanishes (i.e. when either Θ or p_{nc}, the projection of p onto the noncommutative subspace, vanishes), the nonplanar graph is singular at small $|p_\mu\Theta^{\mu\nu}|$. Indeed, the effective cutoff for a one loop graph in momentum space is $\frac{1}{\sqrt{-p_\mu\Theta^2_{\mu\nu}p_\nu}}$ where p is some combination of the external momenta in the process. Therefore turning on Θ replaces the UV divergence with singular IR behavior. This effect has interesting dynamical consequences for noncommutative field theories, some of which are explored below.

3.1. Quadratic Effective action in ϕ^4 theory in $d = 4$

We begin with ϕ^4 theory in four dimensions with the Euclidean action

$$S = \int d^4x \big(\frac{1}{2}(\partial_\mu\phi)^2 + \frac{1}{2}m^2\phi^2 + \frac{1}{4!}g^2\phi\star\phi\star\phi\star\phi\big). \tag{3.1}$$

Consider the $1PI$ two point function, which at lowest order is simply the inverse propagator

$$\Gamma^{(2)}_0 = p^2 + m^2. \tag{3.2}$$

In the noncommutative theory, this receives corrections at one loop from the two diagrams of Fig. 4, one planar and the other non-planar.

Fig. 4: Planar and nonplanar one loop corrections to $\Gamma^{(2)}$ in ϕ^4 theory.

The two diagrams (which are identical in the $\Theta = 0$ theory up to a symmetry factor) give

$$\begin{aligned}\Gamma^{(2)}_{1\ planar} &= \frac{g^2}{3(2\pi)^4}\int\frac{d^4k}{k^2+m^2}\\ \Gamma^{(2)}_{1\ nonplanar} &= \frac{g^2}{6(2\pi)^4}\int\frac{d^4k}{k^2+m^2}e^{ik\times p}\end{aligned} \tag{3.3}$$

The planar diagram is proportional to the one loop mass correction of the commutative theory, and is quadratically divergent at high energies. In order to see the effect of the phase factor in the second integral we rewrite the expressions for the two integrals in terms of Schwinger parameters

$$\frac{1}{k^2+m^2} = \int_0^\infty d\alpha\ e^{-\alpha(k^2+m^2)}. \tag{3.4}$$

The k integrals are now Gaussian, and may be evaluated to yield

$$\begin{aligned} \Gamma^{(2)}_{1\ planar} &= \frac{g^2}{48\pi^2}\int \frac{d\alpha}{\alpha^2} e^{-\alpha m^2} \\ \Gamma^{(2)}_{1\ nonplanar} &= \frac{g^2}{96\pi^2}\int \frac{d\alpha}{\alpha^2} e^{-\alpha m^2 - \frac{p\circ p}{\alpha}}, \end{aligned} \tag{3.5}$$

where we have introduced new notation

$$p\circ q \equiv -p_\mu \Theta^2_{\mu\nu} q_\nu = |p_\mu \Theta^2_{\mu\nu} q_\nu| \tag{3.6}$$

(note that $p\circ p$ has dimension of length squared). In order to regulate the small α divergence in (3.5) we multiply the integrands in the expressions above by $exp(-1/(\Lambda^2\alpha))$ to get

$$\begin{aligned} \Gamma^{(2)}_{1\ planar} &= \frac{g^2}{48\pi^2}\int \frac{d\alpha}{\alpha^2} e^{-\alpha m^2 - \frac{1}{\Lambda^2\alpha}} \\ \Gamma^{(2)}_{1\ nonplanar} &= \frac{g^2}{96\pi^2}\int \frac{d\alpha}{\alpha^2} e^{-\alpha m^2 - \frac{p\circ p + \frac{1}{\Lambda^2}}{\alpha}}. \end{aligned} \tag{3.7}$$

Therefore,

$$\begin{aligned} \Gamma^{(2)}_{1\ planar} &= \frac{g^2}{48\pi^2}\big(\Lambda^2 - m^2 \ln(\frac{\Lambda^2}{m^2}) + O(1)\big) \\ \Gamma^{(2)}_{1\ nonplanar} &= \frac{g^2}{96\pi^2}\big(\Lambda^2_{eff} - m^2 \ln(\frac{\Lambda^2_{eff}}{m^2}) + O(1)\big), \end{aligned} \tag{3.8}$$

where

$$\Lambda^2_{eff} = \frac{1}{1/\Lambda^2 + p\circ p}. \tag{3.9}$$

In the limit $\Lambda\to\infty$, the nonplanar one loop graph remains finite, effectively regulated by the noncommutativity of spacetime. In this limit the effective cutoff $\Lambda^2_{eff} = \frac{1}{p\circ p}$ goes to infinity when either $\Theta\to 0$ or $p_{nc}\to 0$.

The one loop 1PI quadratic effective action is

$$\begin{aligned} S^{(2)}_{1PI} = \int d^4p \frac{1}{2}\Big(p^2 + M^2 + \frac{g^2}{96\pi^2(p\circ p + \frac{1}{\Lambda^2})} - \frac{g^2M^2}{96\pi^2}\ln\left(\frac{1}{M^2(p\circ p + \frac{1}{\Lambda^2})}\right) + \\ \cdots + \mathcal{O}(g^4)\Big)\phi(p)\phi(-p) \end{aligned} \tag{3.10}$$

where $M^2 = m^2 + \frac{g^2\Lambda^2}{48\pi^2} - \frac{g^2m^2}{48\pi^2}\ln\left(\frac{\Lambda^2}{m^2}\right)$ ... is the renormalized mass. Consider the two cases

a) $p \circ p \ll \frac{1}{\Lambda^2}$, and in particular the zero momentum limit. Here $\Lambda_{eff} \approx \Lambda$, and we recover the effective action of the commutative theory,

$$S^{(2)}_{1PI} = \int d^4p \frac{1}{2}\left(p^2 + M'^2\right)\phi(p)\phi(-p), \tag{3.11}$$

where $M'^2 = M^2 + 3\frac{g^2\Lambda^2}{96\pi^2} - \frac{3g^2m^2}{96\pi^2}\ln\left(\frac{\Lambda^2}{m^2}\right)$ ... . If M is fine tuned to be cutoff independent, then M' and also $S^{(2)}_{1PI}$ diverge as $\Lambda\to\infty$.

b) $p \circ p \gg \frac{1}{\Lambda^2}$ and in particular the limit $\Lambda\to\infty$. Here $\Lambda^2_{eff} = \frac{1}{p\circ p}$, and

$$\begin{aligned} S_{eff} = \int d^4p \frac{1}{2}\Big(p^2 + M^2 + \frac{g^2}{96\pi^2 p\circ p} \\ - \frac{g^2M^2}{96\pi^2}\ln\left(\frac{1}{m^2 p\circ p}\right) + ... + \ \mathcal{O}(g^4)\Big)\phi(p)\phi(-p). \end{aligned} \tag{3.12}$$

The fact that the limit $\Lambda\to\infty$ does not commute with the low momentum limit $p_{nc}\to 0$ demonstrates the interesting mixing of the UV ($\Lambda\to 0$) and IR ($p\to 0$) in this theory. We will say more about this below.

3.2. Quadratic effective action in ϕ^3 theory in $d = 6$

We repeat the computation performed above for ϕ^3 theory in six dimensions. Apart from a crucial sign, our results will mimic those of the previous subsection.

Let

$$S = \int d^6x\big(\frac{1}{2}(\partial_\mu\phi)^2 + \frac{1}{2}m^2\phi^2 + \frac{g}{3!}\phi\star\phi\star\phi\big). \tag{3.13}$$

As in ϕ^4 theory, $\Gamma^{(2)}$ receives contributions both from a one loop planar and a one loop nonplanar diagram (Fig. 5).

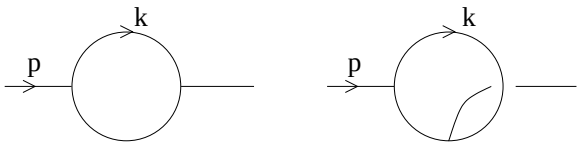

Fig. 5: Planar and nonplanar one loop corrections to $\Gamma^{(2)}$ in ϕ^3 theory.

The contribution of the nonplanar diagram may be written as an integral over Schwinger parameters as

$$\begin{aligned}\Gamma^{(2)}_{1\ nonplanar} &= -\frac{g^2}{2^8\pi^3}\int \frac{d\alpha_1 d\alpha_2}{(\alpha_1+\alpha_2)^3} e^{-m^2(\alpha_1+\alpha_2)-\frac{p^2\alpha_1\alpha_2}{\alpha_1+\alpha_2}-\frac{p\circ p+\frac{1}{\Lambda^2}}{\alpha_1+\alpha_2}} \\ \Gamma^{(2)}_{1\ planar} &= \Gamma^{(2)}_{1\ nonplanar}(\Theta=0).\end{aligned} \tag{3.14}$$

The planar graph has a quadratic divergence from the region where both α's are small. As above, this divergence is effectively cutoff in the nonplanar graph, producing a ($\Lambda\to\infty$) quadratic effective action

$$S^{(2)}_{1PI} = \int d^6p \frac{1}{2}\left(p^2+M^2-\frac{g^2}{2^8\pi^2 p\circ p}+\frac{g^2}{2^9 3\pi^3}(p^2+6M^2)\ln(\frac{1}{M^2 p\circ p})+...\right)\phi_R(p)\phi_R(-p), \tag{3.15}$$

where M is the planar renormalized mass, and ϕ_R the planar renormalized scalar field.

3.3. Validity of the 1-loop approximation

Although nonplanar contributions to (3.12) and (3.15) are subleading in g^2, they are singular as $p_{nc}\to 0$, and so cannot be ignored. In particular, the nonplanar term significantly modifies $S^{(2)}_{1PI}$ for $(p^2+M^2)p\circ p < \mathcal{O}(g^2)$.

Since the singular dependence of $\Gamma^{(2)}_{nonplanar}$ on $p\circ p$ replaces the divergent dependence of $\Gamma^{(2)}$ on Λ at $\Theta=0$, the leading singularity in $\Gamma^{(2)}_{nonplanar}$ at n^{th} order in perturbation theory is $g^{2n}\frac{1}{p\circ p}\left(\ln(p\circ pM^2)\right)^{n-1}$ (we will study $n=2$ in section 5). These higher order contributions are significant when compared to the first order effect only for momenta such that $g^{2n}\frac{1}{p\circ p}\left(\ln\left(p\circ pM^2\right)\right)^{n-1}\approx\frac{g^2}{p\circ p}$, i.e. for $M^2 p\circ p\leq\mathcal{O}(e^{-\frac{c}{g^2}})$ (c is a positive constant). Thus the 1-loop approximation to $\Gamma^{(2)}_{nonplanar}$ is both important and valid for

$$\mathcal{O}(e^{-\frac{c}{g^2}})\leq M^2(p\circ p)\leq\mathcal{O}(g^2). \tag{3.16}$$

The p dependence can be trusted at low momentum except for nonperturbatively small values of p.

3.4. Stability of the Perturbative Vacuum: with and without Fermions

Both (3.12) and (3.15) take the form

$$S^{(2)}_{1PI} = \int d^6p\frac{1}{2}\phi(p)\phi(-p)(p^2+M^2+h\frac{g^2}{p\circ p}+\{\text{subleading}\}). \tag{3.17}$$

The constant h is positive for the ϕ^4 theory in $d = 4$, but negative for the ϕ^3 theory in $d = 6$, leading to a qualitative difference between the dynamics of the two examples.

When h is positive, the coefficient of $|\phi(p)|^2$ in (3.17) is positive for all p. The nonplanar one loop contribution to (3.17) modifies the ϕ propagator at small momenta, inducing long range interactions (see the next subsection).

When h is negative, the coefficient of $|\phi(p)|^2$ in (3.17) is negative for momenta so small that $(p^2 + M^2)p \circ p < \mathcal{O}(g^2)$. In order to minimize the effective action, $\phi(p)$ attains a vacuum expectation value, at these low momenta. In other words, the perturbative vacuum is unstable.

Since the perturbative vacuum for ϕ^3 theory is unstable anyway, the observation of the previous paragraph may not seem too dramatic. However, a similar effect occurs in a suitably modified ϕ^4 theory in four dimensions. Recall that the term $\frac{hg^2}{p \circ p}$ in (3.17) results from the quadratic divergence of the nonplanar diagram of the commutative theory. The sign of the infrared pole is therefore correlated with the sign of the mass renormalization (due to nonplanar graphs) of this theory.

Now adding sufficiently many (or sufficiently strongly) Yukawa coupled fermions to the ϕ^4 theory changes the sign of the mass renormalization. (Recall that a model with a single complex scalar and a single chiral fermion with Yukawa coupling g is supersymmetric, has no quadratic divergences, and therefore $h = 0$.) Thus, in such a theory the sign of the $p \circ p$ leads to an instability and the low energy theory has to be analyzed carefully. We will return to this problem below.

3.5. Poles in the Propagator

The propagator derived from (3.17) has two poles. The first is the continuation to weak coupling of the zero coupling pole at $p^2 + m^2 = 0$, and occurs at

$$p^2 + m^2 = \mathcal{O}(g^2). \tag{3.18}$$

It corresponds to the fundamental ϕ quanta. The second is absent at zero coupling and occurs at

$$p \circ p = -\frac{g^2 h}{p_c^2 + m^2} + \mathcal{O}(g^4), \tag{3.19}$$

where p_c is the restriction of p to the commutative subspace ($p_c = 0$ if Θ is of maximal rank).

The second pole (3.19) formally signals the presence of a new 'particle' (we will qualify this below), whose mass goes to zero as g^2 is taken to zero. This is true even though the theory is massive, with mass m. In fact, m plays no significant role in the new pole.

The appearance of the second pole in the ϕ propagator might make one wonder if the nonlocality of the tree level noncommutative action was a consequence of a massless particle having been integrated out. We do not believe this is the case. Integrating out a massless particle produces a nonlocal Lagrangian that is nonanalytic in momenta around $p = 0$, while the noncommutative action is completely analytic in momenta at all p. Indeed, the low momentum singularity in the effective action results from integrating out very high (rather than very low) momenta. The light mode in the propagator is a consequence of very high energy dynamics!

In Euclidean space, in the limit $g^2 \to 0$, both poles in the propagator occur at imaginary values of momenta (in the case $h > 0$). In Lorentzian signature, we have to choose $\Theta^{0i} = 0$. Then $p^2 + m^2 = 0$ can be satisfied with real momenta, but $p \circ p = 0$ cannot (except for the trivial solution $p_{nc} = 0$). Thus the second pole corresponds to a Lagrange multiplier, rather than a propagating particle.

At small finite values of g^2, $p \circ p = -\frac{g^2 h}{p_c^2 + m^2}$ can be satisfied by real momenta in *Euclidean* space if and only if h is negative. A pole at real values of Euclidean momenta corresponds to a tachyonic instability of the vacuum, in accord with the discussion of the previous subsection. As discussed there, the sign of h depends on the details of the theory.

The pole in the propagator at small values of p has dramatic consequences. In position space it leads to long range correlations. Normally correlation functions decay exponentially, with the decay constant given by the mass m. In the noncommutative theory, with Θ of maximum rank, they decay algebraically for small g, and the small g corrections lead to exponential decay, but with decay constant of order g. We should stress that all this is only for positive h. Otherwise, the theory is tachyonic and suffers from the instability discussed above.

3.6. Wilsonian Lagrangian

Consider a Wilsonian action with a cutoff Λ, of the form

$$S_{eff}(\Lambda) = \int d^4x \frac{Z(\Lambda)}{2} \left((\partial\phi)^2 + m^2(\Lambda)\phi^2 \right) + \frac{g^2(\Lambda) Z^2(\Lambda)}{4!} (\phi \star \phi \star \phi \star \phi). \tag{3.20}$$

The statement that the noncommutative ϕ^4 theory is renormalizable would normally imply that it is possible to choose the functions $Z(\Lambda)$, $m(\Lambda)$ and $g^2(\Lambda)$ in such a way that

a) Correlation functions computed with this Lagrangian have a limit as $\Lambda \to \infty$.

b) Correlation functions computed at finite Λ differ from their limiting values by terms of order $\frac{1}{\Lambda}$ for all values of momenta.

Property b) is manifestly untrue of the noncommutative scalar theories under consideration. While it is presumably possible to choose $Z(\Lambda)$, $m(\Lambda)$ and $g^2(\Lambda)$ in such a way that the $\Lambda \to \infty$ limit of all correlation functions exists, the various correlation functions (at various values of momenta) do not converge uniformly to their limiting values. As we have seen above, the two point function computed using (3.20) at any finite value of Λ differs significantly from its $\Lambda \to \infty$ value for small enough momentum p_{nc} (for $p \circ p \Lambda^2 \ll 1$). In particular, as we have noted previously, the limit $p_{nc} \to 0$ does not commute with the limit $\Lambda \to \infty$.

We attempt to find a substitute for (3.20) which correctly captures the leading small momentum singularity in $\langle \phi\phi \rangle$ at finite Λ. To this end we introduce a new degree of freedom into the Wilsonian action, that reproduces the important low energy effects arising from integrating out the modes between Λ and ∞. The new degree of freedom should give a contribution to the $\phi\phi$ two point function that is small for $p \circ p \Lambda^2 \gg 1$ and is approximately $\frac{1}{p \circ p}$ for $p \circ p \Lambda^2 \ll 1$. This is achieved by introducing a new field χ into the modified Wilsonian action

$$S'_{eff}(\Lambda) = S_{eff}(\Lambda) + \int d^4x \left(\frac{1}{2} \partial\chi \circ \partial\chi + \frac{1}{2} \Lambda^2 \left(\partial \circ \partial \chi \right)^2 + i \frac{1}{\sqrt{96\pi^2}} g \chi \phi \right). \tag{3.21}$$

χ appears quadratically in (3.21) and so may be integrated out, yielding

$$S'_{eff}(\Lambda) = S_{eff}(\Lambda) + \int \frac{d^4p}{2} \phi(p)\phi(-p) \frac{1}{96\pi^2} \left(\frac{g^2}{p \circ p} - \frac{g^2}{p \circ p + \frac{1}{\Lambda^2}} \right). \tag{3.22}$$

As we have seen above, S_{eff} leads to the quadratic 1PI effective action (3.10) at $\mathcal{O}(g^2)$. Therefore, the quadratic 1PI effective action at $\mathcal{O}(g^2)$ resulting from S'_{eff} is

$$S_{1PI} = \int \frac{d^4p}{2} \left(p^2 + M^2 + \frac{g^2}{96\pi^2 p \circ p} + \frac{g^2 M^2}{96\pi^2} \ln \left(\frac{1}{M^2 (p \circ p + \frac{1}{\Lambda^2})} \right) + \cdots \right) \phi(p)\phi(-p) \tag{3.23}$$

correctly reproducing the leading low momentum singularity of the true 1PI effective action (3.12) but incorrectly cutting off the logarithmic singularity.

3.7. Logarithms

So far the effects we have been discussing arose from what started as quadratic divergences in the commutative theory. These turned into poles, $\frac{1}{p\circ p}$, in the noncommutative theory, which we interpreted as the χ pole in the Wilsonian action. Logarithmic divergences are more common than quadratic divergences. They occur even when the quadratic divergences are absent as is the case in supersymmetric theories or in gauge theories. They also occur in the scalar theories which we have been discussing.

The logarithmic UV divergences in the nonplanar graphs of the commutative theory turn into terms of the form $\ln p \circ p$, which are nonanalytic around $p = 0$. Rather than a pole, $\frac{1}{p\circ p}$, we now have a cut, $\ln p \circ p$, which is also an IR singularity.

Unfortunately, we do not fully understand the implications of the logarithmic singularity in (3.12). Consider the Wilsonian effective action at small Λ. The dynamics of ϕ freezes out at these energies (as ϕ is massive), and so ϕ is effectively classical. χ is a free light quantum field (its four derivative kinetic term is negligible at low energies). The low energy Wilsonian effective action should correctly reproduce the low energy correlation functions of ϕ. The effective action (3.21) (which is expected to be correct for large Λ) cannot accurately approximate the small Λ effective action, because correlation functions computed using (3.21) at small Λ correctly reproduce the pole but do not reproduce the logarithm. The correct small Λ effective action must contain new dynamics, absent in (3.21). We see two possibilities for the missing dynamics:

a) The classical field ϕ can couple to two massless particles, resulting in a cut in its two point function.

b) The classical field ϕ can couple to a low energy conformal field theory, with operators of dimensions of order g^2; the logarithm represents the first term in the expansion of $\left(p \circ pm^2\right)^{cg^2+\cdots}$.

Clearly, these logarithms need better understanding. We should point out, however, that regardless of the details, just like the poles, they demonstrate an IR singularity due to a UV phenomenon!

3.8. Vertex corrections

We end this section with a brief look at the contribution of one loop nonplanar graphs to vertex corrections. The graphs we will compute are logarithmically divergent in the commutative theory, and so will depend logarithmically on $p^i \circ p^j$, where p^i and p^j are

external momenta. Since we are primarily interested in low momentum singularities, we will ignore all terms regular in p^i at $p^i = 0$. In particular, external momentum dependent phase factors that factor out of the integral will be ignored.

Noncommutative ϕ^3 in six dimensions

Eight graphs contribute to the one loop vertex correction in ϕ^3 theory in six dimensions. Two of these are planar, (e.g. the first graph in Fig. 6), and differ in the cyclic ordering of external lines. The remaining six graphs are nonplanar (e.g. the second graph in Fig. 6), and differ in the choice of the external line that cuts an internal line (3 choices), as well as the cyclic ordering of external lines, given this choice (2 choices). Graphs that differ only in the cyclic ordering of external lines differ only by an external momentum dependent phase factor. For small external momenta, these phases are unimportant, so the one loop vertex correction receives four distinct contributions, each with symmetry factor $\frac{1}{4}$.

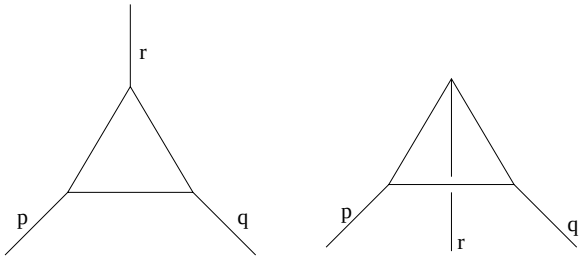

Fig. 6: Planar and nonplanar one loop corrections to $\Gamma^{(3)}$ in ϕ^3 theory.

In this approximation, the nonplanar graph shown in Fig. 6, in terms of Schwinger parameters, gives

$$\frac{1}{2^6\pi^3}\int \frac{d\alpha d\beta d\gamma}{(\alpha+\beta+\gamma)^3} e^{-\frac{r\circ r+\frac{1}{\Lambda^2}}{\alpha+\beta+\gamma}-m^2(\alpha+\beta+\gamma)}. \tag{3.24}$$

The planar graph is given by the same expression, but with Θ set to zero. The logarithmic divergence of the planar graph is effectively cutoff in the nonplanar graph by $\Lambda^2_{eff}(r) = \frac{1}{r\circ r+\frac{1}{\Lambda^2}}$. Summing up the contribution of the graphs, in the limit $\Lambda\to\infty$, we find

$$\Gamma^{(3)} = g + \frac{g^3}{2^9\pi^3}\left\{ln\left(\frac{\Lambda^2}{m^2}\right) + ln\left(\frac{1}{m^2 p\circ p}\right) + \ln\left(\frac{1}{m^2 q\circ q}\right) + ln\left(\frac{1}{m^2 r\circ r}\right)\right\} + \dots \tag{3.25}$$

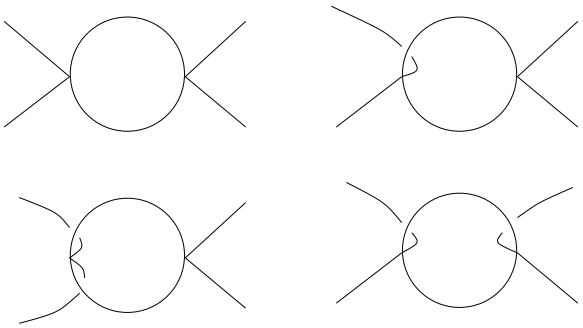

Fig. 7: Planar and nonplanar one loop corrections to $\Gamma^{(4)}$ in ϕ^4 theory.

Noncommutative ϕ^4 in four dimensions

The graphs that contribute to the 1-loop renormalization of the coupling constant in ϕ^4 theory are shown schematically in Fig. 7.
For small external momenta we find

$$\Gamma^{(4)} = g^2 - \frac{g^4}{3\cdot 2^5\,\pi^2}\left\{2ln\left(\frac{\Lambda^2}{m^2}\right) + ln\left(\frac{1}{m^2 p\circ p}\right) + ln\left(\frac{1}{m^2 q\circ q}\right) + ln\left(\frac{1}{m^2 r\circ r}\right) + ln\left(\frac{1}{m^2 s\circ s}\right) + ln\left(\frac{1}{m^2 (q+r)\circ (q+r)}\right) + ln\left(\frac{1}{m^2 (q+s)\circ (q+s)}\right) + ln\left(\frac{1}{m^2 (r+s)\circ (r+s)}\right)\right\} + \dots \tag{3.26}$$

For both ϕ^4 and ϕ^3 theories, each nonplanar graph has an effective cutoff $1/P\circ P$ where P is the combination of external momenta which crosses the loop.

4. A Stringy Analogue

Consider the nonplanar one loop mass correction diagram for ϕ^3 theory, shown in Fig. 5. This diagram may be redrawn in double line notation, as in Fig. 8. Of course, in the noncommutative field theory, Fig. 8 represents a *particle* running in the loop and the double line has no thickness.

Consider, however, the 1-loop open string diagram (called the double twist diagram) that may also be drawn as in Fig. 8. In string perturbation theory we integrate over the moduli of the diagrams. The region of moduli space that corresponds to high energies in the open string loop describes also the tree level exchange of a closed string state as in Fig. 9. It leads to a singularity proportional to $\frac{1}{p_\mu g^{\mu\nu} p_\nu}$, ($g$ is the closed string metric). UV in the open string channel corresponds to IR in the closed string channel.

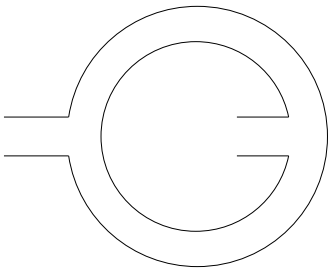

Fig. 8: The nonplanar mass correction graph for ϕ^3 theory redrawn in double line notation.

Fig. 9: The double twist diagram in the closed string channel.

This matches exactly with the behavior of the field theory diagram of Fig. 8, if we identify the closed string metric as being proportional to $-\Theta^2_{\mu\nu}$. In fact this identification is very natural. In [14], it was emphasized that the analysis of D-branes in the presence of a B field involves two metrics that are related to each other. The noncommutative gauge theory propagating on the brane "sees" the open string metric. The closed string metric governs the propagation of closed string states in the bulk. When the open string metric is the identity (as in our paper), the closed string metric reduces (in the decoupling limit) to $-\alpha'\Theta^2_{\mu\nu}$!

This close analogy between a one loop effect in a rather ordinary looking (though nonlocal) field theory and an open string theory is quite surprising, and is not completely understood. It is an indication of the stringy behavior of noncommutative field theories. Other hints of the stringy nature of noncommutative theories are the T-duality symmetry of noncommutative gauge theories on tori, and the dominance of planar graphs in a perturbative expansion at high momentum. We will elaborate on these in section 7.

5. Higher Order Diagrams

In this section we examine the effects of noncommutativity in higher order nonplanar diagrams. In subsection 5.1 we find examples of nonplanar diagrams (in scalar field

theories) that diverge, and interpret these as IR divergences. In subsection 5.2 we illustrate various other effects of noncommutativity at higher orders in a two loop example. In subsection 5.3 we present the expression for the Feynman integral of an arbitrary noncommutative diagram in the Schwinger parameter representation, and comment on the structural features of this formula. Finally in subsection 5.4, we point out the stringy nature of 'maximally noncommutative' theories obtained by taking $\Theta \to \infty$.

5.1. Persistence of divergences in some nonplanar graphs

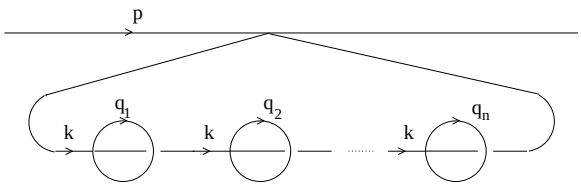

Fig. 10: Divergent higher loop graphs in ϕ^4 theory.

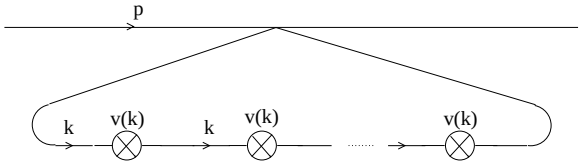

Fig. 11: An equivalent way of representing the Feynman integral for the graph of Fig. 10. The mass like vertex $v(k)$ for this graph has been computed in section 3.

Consider the diagram G of Fig. 10 in noncommutative ϕ^4 theory in four dimensions. This graph has n insertions of the nonplanar one loop mass correction that we have computed in (3.8), and so may equivalently be represented as in Fig. 11, where

$$v(k) = -\frac{g^2}{96\pi^2}\frac{1}{k \circ k + \frac{1}{\Lambda^2}} + \ less\ singular. \tag{5.1}$$

The Feynman integral for the diagram is

$$\mathcal{I}(G) = \frac{1}{(2\pi)^4}\int d^4k \frac{[v(k)]^n}{(m^2+k^2)^{n+1}} \tag{5.2}$$

The contribution to $\mathcal{I}(G)$ from the infrared singularities of $v(k)$ is proportional to

$$\int \frac{d^r k_{nc}}{(k \circ k + \frac{1}{\Lambda^2})^n} \propto \begin{cases} \Lambda^{2n-r} & 2n \geq r \\ const & 2n < r \end{cases} \tag{5.3}$$

(k_{nc} is the projection of k on the noncommuting subspace in the case where the rank r of Θ is not maximal). As $\Lambda \to \infty$, $\mathcal{I}(G)$ diverges for $n \geq [r/2]$. This divergence occurs at small k_{nc}, and high q_i in the loops of Fig. 10. It is a combination of UV and IR divergence. The presence of an IR divergence in a massive theory is surprising, but is in accord with the other IR phenomena we have seen earlier.

If we first integrate over k, the divergence in $\mathcal{I}(G)$ appears like a UV divergence in the integrals over q_i. If, however, we first integrate over q_i, the divergence appears like an IR divergence in the integral over k. We prefer the latter interpretation, and propose to deal with the divergence in $\mathcal{I}(G)$ in a fashion similar to the standard treatment of IR divergences.

We postpone the integral over k and first sum over n to shift the location of the pole in the propagator to be outside the integration region. More specifically, summing the infinite series of increasingly divergent graphs of Fig. 10 for all n as in Fig 12, (and also including planar one loop mass corrections) yields

$$\mathcal{I} = \int \frac{d^4k}{\Gamma^{(2)}(k)}, \tag{5.4}$$

where $\Gamma^{(2)}(k)$ is derived from (3.12) and is given by

$$\Gamma^2(k) = M^2 + k^2 + \frac{g^2}{96\pi^2 k \circ k} + \dots \ . \tag{5.5}$$

As a result, the integral over k in (5.4) is finite (up to a standard UV divergence).

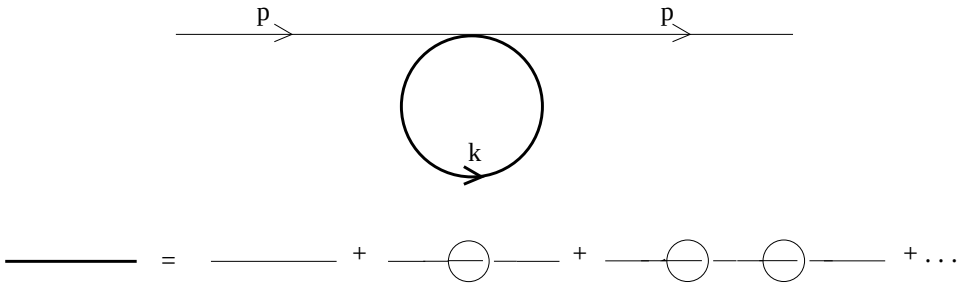

Fig. 12: An infinite series of divergent graphs sums up to a single graph with the dressed one loop propagator.

This procedure cannot be used in theories with negative h because the dangerous pole in the propagator is shifted to become tachyonic. Then, the proper procedure is to compute the low energy effective action of the χ field and to find its minimum. We will not attempt to perform such a calculation here.

We suggest that UV divergences occur only in planar graphs and all other divergences can be treated as IR divergences, yielding finite, physically sensible answers. We have not proved this assertion. It will be very interesting to have an explicit proof of this fact.

5.2. Other effects at two loops

In this subsection we examine all two loop graphs that contribute to the self mass of (for simplicity) ϕ^3 theory in six dimensions. This will illustrate further effect of noncommutativity present in higher order graphs.

Noncommutative ϕ^3 theory in six dimensions has two classes of mass correction graphs at two loops, corresponding to the two graphs in the ordinary ϕ^3 theory shown in Fig. 13.

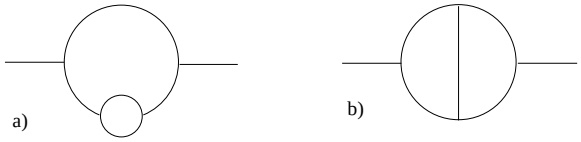

Fig. 13: The two loop contributions to the self mass of commutative ϕ^3 theory in six dimensions.

Diagrams in the first class reduce to the graph of Fig. 13a at $\Theta = 0$. These diagrams are members of an infinite set of graphs that correct the propagators in the graphs of Fig. 5, as in the previous subsection. The analysis of these graphs parallels that given in the previous section for the ϕ^4 theory.

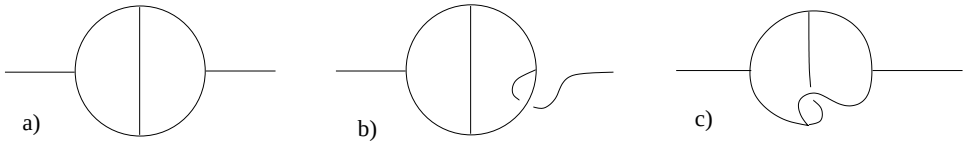

Fig. 14: Representatives of the three categories of graphs in noncommutative ϕ^3 theory that reduce to the diagram of Fig. 13b at $\Theta = 0$.

The diagrams that reduce to the graph of Fig. 13b at $\Theta = 0$ fall into three categories, representatives of which are shown in Fig. 14. Fig. 14a shows the single planar graph. The corresponding Feynman integral does not depend on Θ, and evaluates to $\frac{1}{8}$ times the result for the graph of Fig. 13b in the commutative theory. As in the commutative theory, this graph contains overlapping divergences. These are dealt with in the usual way, by combining it with the counterterm graphs of Fig. 15a and Fig. 15b, whose contributions are also suppressed by a factor $\frac{1}{8}$ relative to the commutative theory. Thus, as in the commutative theory, the graphs of Figs. 14a, 15a and 15b combine to give a result whose divergence may be cancelled by counterterms.

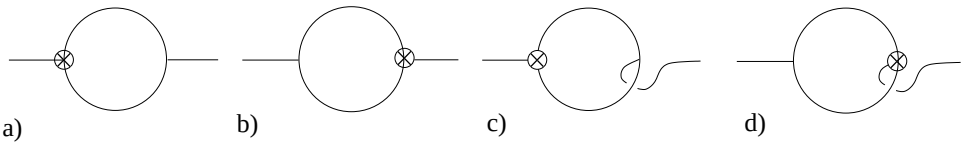

Fig. 15: One loop mass correction graphs with one loop vertex correction counterterms.

Fig. 14b represents a set of three nonplanar graphs, each of which is nonplanar only because an external line overlaps with an internal line. Two of these graphs contain divergent planar vertex correction subgraphs and should respectively be combined with the one loop graphs containing counterterms shown in Figs. 15c and 15d. Once their subdiagrams have been renormalized, these diagrams, as well as the third diagram in this set, are finite, effectively cut off by $\Lambda_{eff} = \frac{1}{\sqrt{p \circ p}}$. At large Λ_{eff}, these graphs are all proportional to $g^4 \Lambda_{eff}^2 \ln(\Lambda_{eff})$, providing a logarithmic correction to the leading singularity in (3.15). The proportionality of these diagrams to $\Lambda_{eff}^2 \ln(\Lambda_{eff})$ (rather than Λ_{eff}^2) is a consequence of the fact that fewer counterterms are added in the noncommutative theory than in the commutative theory.

The four remaining two loop mass correction graphs, which include the diagram of Fig. 14c, are nonplanar due to the crossing of internal lines. As we will show in the next subsection, these graphs are finite, effectively cutoff by $1/\sqrt{\theta}$ where θ is the largest eigenvalue of $\Theta^{\mu\nu}$. In contrast to the nonplanar one loop graphs and the graphs considered in the previous paragraph, these diagrams are nonsingular at low momenta, since the effective cutoff is independent of external momenta. This is a consequence of the fact that the noncommutative phase factor responsible for removing the divergence depends only on internal momenta, which are integrated over.

5.3. General Higher order graphs

In the appendix, we express the Feynman integral for an arbitrary graph (G) in terms of an integral over Schwinger parameters. Up to overall constants, the result (part of which has been independently reported in [11]) is

$$\delta(\sum p_I) V(p^I) \int d\alpha_i e^{-\alpha_i m_i^2} \frac{1}{(\prod_{\theta_a} P_G(\alpha, \theta_a))^{\frac{1}{2}}} e^{-p_\mu^I \left(\frac{S_{IJ}(\alpha, \Theta^2)}{P_G(\alpha, \Theta^2)} \right)^{\mu\nu} p_\nu^J - i p_\mu^I \left(\frac{\Theta A_{IJ}(\alpha, \Theta^2)}{P_G(\alpha, \Theta^2)} \right)^{\mu\nu} p_\nu^J}. \tag{5.6}$$

Here P, S, and A are homogeneous polynomials in $\{\alpha_i, \Theta\}$, described in terms of graph theoretic properties of G in the Appendix, the phase $V(p^I)$ is as in (2.6), and θ_a are the eigenvalues of Θ.

Four terms in this expression involve the noncommutativity parameter Θ:

1) The first factor $V(p^I)$ is the overall phase, present for any graph. It depends on the cyclic order of the external momenta p. This is the sole effect of non-commutativity for planar graphs.
2) The denominator P_G is a homogeneous polynomial in $\{\alpha_i, \Theta\}$ (independent of external momenta) of degree L, where L is the number of loops in G. Divergences of a graph are associated with regions of parameter space where $P_G \to 0$. Crossing internal lines of G give rise to Θ dependent terms in P, and these reduce the rate at which P becomes small when the α's are scaled to zero. More precisely, the degree of P_G as a function of Θ is $2h$, where h is the genus of G (with external lines removed), so a graph with superficial degree of divergence ω at $\Theta = 0$ will essentially have a superficial degree of divergence $\omega - 2hr$ for Θ of rank r. Thus, crossing internal lines regulate the divergences with an effective cutoff of order $\frac{1}{\sqrt{\Theta}}$ (assume for simplicity that Θ has maximal rank and all its entries are of the same order of magnitude), as for the graph of Fig. 14c. In particular, this effective UV cutoff depends only on Θ and not on the momenta.
3) The exponential factor $exp(-p^I_\mu (S_{IJ}/P_G)^{\mu\nu} p^J_\nu)$ acts to reduce divergences when an external momentum p crosses an internal line. If the momenta associated with some subgraph G_q of G crossed by p are scaled by ρ, then the exponential scales as $exp(-p \circ p/\rho)$. Thus the exponential cuts off possible divergences associated with G_q, with an effective cutoff $\frac{1}{\sqrt{p \circ p}}$, as we have seen for the one loop graphs of section 3. As there, this cutoff depends both on Θ and on the momenta and becomes large as $p \circ p \to 0$, resulting in the singular IR behavior we have seen previously.
4) The final exponential factor in (5.6) is a phase in the integrand which depends on the Schwinger parameters. This modifies the behavior of finite graphs, but does not seem to affect the convergence of the graph.

Using these expressions, it is possible to demonstrate the convergence (at $\Theta \neq 0$) of the Feynman integral associated with G, if G has no divergent planar subgraphs and $\omega(G_i) \leq 0$, for all subgraphs G_i of G, where ω denotes the degree of divergence of a graph.

As we have remarked above, the issue of renormalizability of scalar noncommutative field theories is quite subtle. Some nonplanar graphs are divergent, but we have suggested that the divergence should be viewed as an IR divergence and should be handled appropriately. Therefore, we think it will be quite interesting to prove the renormalizability of these theories to all orders.

5.4. Maximal noncommutativity

It is interesting to consider the limit in which we take the noncommutativity parameter Θ to infinity. In this limit the theory is maximally noncommutative. Equivalently, we can hold Θ fixed and scale all the momenta (and masses) to infinity. If the theory had been an ordinary field theory, and it had not had any mass parameters, this would have been the "short distance limit."

From (5.6) it may be seen that in this limit the amplitudes (at generic values of external momenta) are dominated by the planar graphs. For nonplanar graphs in which internal lines cross, the polynomial P_G blows up as $\Theta \to \infty$. For nonplanar graphs in which external lines cross internal lines, the factor S_{IJ}/P_G behaves like a positive power of Θ, so the exponential tends to zero as $\Theta \to \infty$ (for generical external momenta). Only planar graphs, which have no Θ dependence apart from the overall phase, survive the $\Theta \to \infty$ limit.

This observation is extremely interesting. The maximally noncommutative theory, which is obtained in the limit $\Theta \to \infty$ is given by the planar diagrams only. If ϕ is an $N \times N$ matrix the theory in this limit is independent of N. In particular, it is the same as the large N theory. We therefore conclude that in the high momentum or maximal noncommutativity limit, the diagrams become planar and the theory appears to be stringy.

In Section 4 we pointed out the close similarity between the singular IR effects in the nonplanar one loop diagram here and in open string theory. The T-duality of noncommutative Yang-Mills theories on a torus is yet another indication of the stringy nature of noncommutative field theories. Finally, in the large Θ limit the theory becomes a string theory. We find it intriguing that these field theories exhibit so many stringy phenomena.

6. Origin of UV/IR Mixing

In this section we will give some intuitive explanations for why the noncommutativity of spacetime leads to the surprising mixture of UV and IR. Roughly, very small pulses instantaneously spread out very far upon interacting. In this manner very high energy processes have important long distance consequences.

6.1. Nonlocality of the star product

We may rewrite the star product (1.3) of two functions in position space as [1]

$$\big(\phi_1 \star \phi_2\big)(z) = \int d^d z_1 d^d z_2 \phi_1(z_1)\phi_2(z_2)K(z_1, z_2, z) \tag{6.1}$$

with the kernel

$$K(z_1, z_2, z) = \frac{1}{\det(\Theta)} e^{2i(z-z_1)^\mu \Theta^{-1}_{\mu\nu}(z-z_2)^\nu}. \tag{6.2}$$

Since $|K(z_1, z_2, z)|$ is a constant independent of z_1, z_2, z, the star product appears to be infinitely nonlocal. However, the oscillations in the phase of K suppress parts of the integration region. We now make this statement more precise.

Consider for simplicity the case $d = 2$ with coordinates $[x, y] = i\theta$. Let ϕ_1 be a function which has widths of order Δ_{x1} and Δ_{y1} in the x and y directions, and assume that it varies slowly over its domain of support. Then, the integral over x_1 in (6.1) is proportional to

$$\int dx_1 \phi_1(x_1, y_1) e^{ix_1(y_2-y)/\theta}. \tag{6.3}$$

It is suppressed by phase oscillations if

$$\Delta_{x1}|y_2 - y|/\theta \gg 1. \tag{6.4}$$

We conclude that $(\phi_1 \star \phi_2)(x, y)$ samples ϕ_2 in a width $\delta y_2 \approx \frac{\theta}{\Delta_{1x}}$ about y.

In a similar way we arrive at the estimates

$$\delta y_2 \Delta_{1x} \approx \theta, \quad \delta y_1 \Delta_{2x} \approx \theta, \quad \delta x_2 \Delta_{1y} \approx \theta, \quad \delta x_1 \Delta_{2y} \approx \theta, \tag{6.5}$$

where Δ_{ai} is the width of ϕ_a in the i direction and δ_{ai} is an estimate of the nonlocal width of the a^{th} function sampled by the star product in the i^{th} direction. This is illustrated for Gaussian wave packets in Fig. 16.

For the important special case $\phi_1 = \phi_2 = \phi$, where ϕ is smooth and of width Δ_x, Δ_y, the widths δ_x and δ_y of $\phi \star \phi$ are given by

$$\delta_x \approx max(\Delta_x, \frac{\theta}{\Delta_y}), \quad \delta_y \approx \max(\Delta_y, \frac{\theta}{\Delta_y}). \tag{6.6}$$

Thus if ϕ is nonzero over a very small region of size $\Delta \ll \sqrt{\theta}$, $\phi \star \phi$ is nonzero over a much larger region of size $\frac{\theta}{\Delta}$. This nonlocality has important consequences for the dynamics.

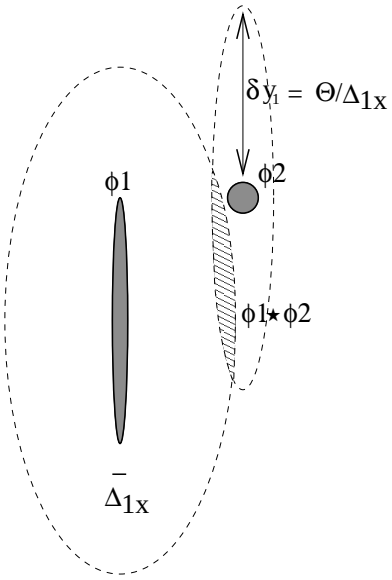

Fig. 16: Star product of Gaussian wave packets ϕ_1 and ϕ_2. If ϕ_1 and ϕ_2 are nonzero only in the shaded regions of the diagram, $(\phi_1 \star \phi_2)$ is nonzero in the intersection of the dotted regions of the diagram. The dotted regions are constructed as described in the text.

6.2. Consequences for Dynamics

Consider, for example, noncommutative ϕ^3 theory (3.13). Classically, $\phi(x)$ obeys the equation

$$\left(\partial^2 - m^2\right)\phi(x) = \frac{g}{2}\left(\phi \star \phi\right)(x). \tag{6.7}$$

Given a solution $\phi_0(x)$ to the free equation of motion, the corresponding solution to (6.7) is given perturbatively by

$$\phi(x) = \phi_0(x) - \frac{g}{2}\int d^d y G(x-y)\left(\phi_0 \star \phi_0\right)(y) + ... \tag{6.8}$$

where $G(x)$ is the appropriate Green's function. At first order the effective source is $\frac{-g}{2}\left(\phi \star \phi\right)(x)$.

As demonstrated in the previous subsection, if $\phi_0(x)$ is nonzero over a region of size Δ, $\left(\phi_0 \star \phi_0\right)(x)$ is nonzero over a region of size $\delta = \max(\Delta, \frac{\theta}{\Delta})$ (θ is a typical entry of the matrix Θ). δ is very big when Δ is very small. Thus, classically, pulses of size $\Delta \ll \sqrt{\theta}$ spread to size $\delta = \frac{\theta}{\Delta} \gg \sqrt{\theta}$ upon interacting. The extent of the spread is independent of the mass of the particle.

In the quantum theory, even very low energy processes receive contributions from high energy virtual particles. In a nonplanar graph, a virtual particle of energy $\omega \gg \frac{1}{\sqrt{\theta}}$ (size

$\frac{1}{\omega} \ll \sqrt{\theta}$) will, upon interacting, spread to size $\omega\theta$, producing important effects at energy $\frac{1}{\theta\omega}$. Therefore, imposing a UV cutoff Λ on ω effectively imposes an IR cutoff $\Lambda_{IR} = \frac{1}{\theta\Lambda}$ on IR singularities produced by the nonplanar graph. Notice that the IR effects produced by high energies in loops are independent of the mass of the particle. This gives us a qualitative explanation for the effects observed in section 3.

7. Noncommutative Yang-Mills

It is difficult to repeat the analysis of the previous sections for gauge theories for several reasons.

a) Noncommutative gauge theories have no local gauge invariant operators. The most easily constructed gauge invariant operators, (for example $\int d^d x Tr \widehat{F}^2$) involve an integration over all space. Approximately local gauge invariant operators may be constructed as follows. Using the change of variables from the noncommutative gauge fields $\widehat{A}$ to the commutative gauge fields A [14] we can construct local gauge invariant operators in terms of A, such as $\mathrm{Tr}F^2$, and express them in terms of the noncommutative variables $\widehat{A}$. These are manifestly gauge invariant, however they are not local. They are given by a power series in Θ and are therefore "smeared" over a region of size of order the only scale in the problem, i.e. $\sqrt{\Theta}$ (again, we assume for simplicity that Θ has maximal rank and all its entries are of the same order of magnitude)[1]. Although such gauge invariant observables exist, it is not clear how to calculate with them and what their properties are. Therefore, it is not clear to what extent the IR effects we encountered above persist in these theories.

b) Noncommutative Yang-Mills theory has massless fields. Thus it is difficult to disentangle the usual IR effects from possible IR singularities induced by the noncommutativity.

c) At low energies, noncommutative gauge theories are strongly coupled in terms of the elementary quanta $\widehat{A}$, and it is not clear what the light degrees of freedom are. Therefore, a low energy effective theory like the one we analyzed in the scalar field theory is not easy to construct.

d) Some of the effects observed in section 3 (for example, the new pole) resulted from the existence of quadratic divergences. Such divergences are absent in Yang-Mills theory

[1] These gauge invariant operators have been suggested by several people among them D. Gross, S. Kachru and E. Silverstein.

which has at worst logarithmic divergences. The logarithmic divergences do lead to IR singularities but they are not as pronounced as the poles we observed and discussed above.

In subsection 7.1 below we present the quadratic one loop 1PI effective action for $U(N)$ noncommutative Yang-Mills. In subsection 7.2 we determine the energy dependence of the dilaton in the string theory dual to noncommutative Yang-Mills, and compare this with the prediction from the AdS/CFT correspondence.

7.1. One Loop in Noncommutative Yang-Mills

The Lagrangian for noncommutative $U(N)$ Yang-Mills theory is given by

$$\mathcal{L} = \frac{1}{4g^2} \int \mathrm{Tr}(\widehat{F}_{\mu\nu}\widehat{F}_{\mu\nu}), \tag{7.1}$$

where $\widehat{A} = \widehat{A}^a t^a$ ($\mathrm{Tr}(t^a t^b) = \delta^{ab}$) and

$$\widehat{F}_{\mu\nu} = \partial_\mu \widehat{A}_\nu - \partial_\nu \widehat{A}_\mu - i\left(\widehat{A}_\mu \star \widehat{A}_\nu - \widehat{A}_\nu \star \widehat{A}_\mu\right) \tag{7.2}$$

is covariant under noncommutative gauge transformations

$$\delta\widehat{A}_\mu = \partial_\mu \epsilon - i\left(\widehat{A}_\mu \star \epsilon - \epsilon \star \widehat{A}_\mu\right) = \widehat{D}_\mu \epsilon. \tag{7.3}$$

Let

$$(\partial\widehat{A})_{\mu\nu} = \partial_\mu \widehat{A}_\nu - \partial_\nu \widehat{A}_\mu. \tag{7.4}$$

The divergent part of the quadratic one loop 1PI effective action of the ordinary $U(N)$ in the background field gauge is given by

$$\Gamma_2^1(\Theta = 0) = \frac{1}{4}\int \left((\frac{1}{g_0^2} + \frac{\beta(g_0^2)}{2g_0^4} \ln \frac{\Lambda_0^2}{k^2})\mathrm{Tr}(\partial A)^2 - \frac{\beta(g_0^2) \ln \frac{\Lambda_0^2}{k^2}}{2g_0^4 N}(Tr\partial A)^2 \right), \tag{7.5}$$

where

$$\beta(g^2) = \frac{-11 g^4 N^2}{12\pi^2} \tag{7.6}$$

is the one loop beta function for $SU(N)$ Yang-Mills, Λ_0 is an ultraviolet cutoff, and g_0 is the bare coupling at scale Λ_0.

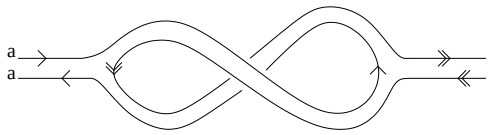

Fig. 17: Nonplanar one loop $U(N)$ diagrams contribute only to the $U(1)$ part of the theory

The only nonplanar contribution to Γ^1 is the term $\frac{1}{4}\int \frac{\beta(g^2)\ln\frac{\Lambda_0^2}{k^2}}{2g_0^4 N}(Tr\partial A)^2$, which receives contributions from diagrams like those of Fig. 17. It contributes only to the $U(1)$ part of the action. In the noncommutative theory, the divergence in this graph will be cut off by $1/\sqrt{p\circ p}$. (Since star products and matrix products always appear together, graphs which are non-planar in the matrix sense will also be nonplanar in the sense we have considered in the rest of this paper.) The divergent part of the quadratic noncommutative one loop effective action is therefore given by

$$\Gamma_2^1 = \frac{1}{4}\int \left((\frac{1}{g_0^2} + \frac{\beta(g_0^2)}{2g_0^4}\ln\frac{\Lambda_0^2}{k^2})\mathrm{Tr}(\partial\widehat{A})^2 - \frac{\beta(g_0^2)\ln\frac{1}{(k\circ k)k^2}}{2g_0^4 N}(\mathrm{Tr}\partial\widehat{A})^2 \right) \tag{7.7}$$

After renormalization,

$$\Gamma_2^1 = \frac{1}{4}\int \left((\frac{1}{g^2(\Lambda)} - \frac{11N}{24\pi^2}\ln\frac{\Lambda^2}{k^2})\mathrm{Tr}(\partial\widehat{A})^2 + \frac{11}{24\pi^2}\ln\frac{1}{k^2(k\circ k)}(\mathrm{Tr}\partial\widehat{A})^2 \right) \tag{7.8}$$

where Λ is an arbitrary finite energy scale, and $g^2(\Lambda)$ is the solution to the equation

$$\frac{dg^2}{d\ln\Lambda} = \beta(g^2) \tag{7.9}$$

with initial condition $g(\Lambda_0) = g_0$.

We make two comments:

a) The one loop beta function for noncommutative $U(N)$ Yang Mills is given for all N, including $N = 1$, by (7.6). Note, in particular, that the $N = 1$ theory is also asymptotically free. The computations in [4-5] confirm (7.6) for $N = 1$. We stress that the beta function for the noncommutative theory can be found without doing any new calculation by simply using the known value of the beta function of the ordinary commutative $SU(N)$ theory.

b) The $U(1)$ part of the quadratic effective action has a logarithmic IR singular piece. This is similar to the the wavefunction 'renormalization' in (3.15). Note that, as for the scalar theory, this one loop logarithm is significantly corrected by higher order effects at energies for which it is important.

7.2. Energy Dependence of the Dilaton

As we have argued in section 5.4, noncommutative theories are dominated by planar graphs, and therefore seem stringy as $\Theta \to \infty$. Specifically, by the formulae of section 5.3, a noncommutative Feynman diagram of genus h (ignoring external lines) is suppressed relative to a planar graph by the factor of

$$\frac{1}{N^{2h}} \prod_{i=1}^{\frac{r}{2}} \frac{1}{(E^2\theta_i)^{2h}}, \tag{7.10}$$

where r is the rank of Θ, whose eigenvalues are $\{\theta_1, -\theta_1 ..., -\theta_r\}$. The contribution of genus h graphs to the $U(N)$ noncommutative gauge theory is expected to reflect the contribution of genus h worldsheets of the 'noncommutative QCD string', whose dilaton ϕ must therefore scale with energy according to

$$e^{-\phi(E)} \propto \frac{1}{N} \prod_{i=1}^{\frac{r}{2}} \frac{1}{E^2\theta_i}. \tag{7.11}$$

This prediction may be tested[2] for the $\mathcal{N} = 4$ noncommutative $U(N)$ theory. The string theory dual to $\mathcal{N} = 4$ noncommutative $U(N)$ is IIB theory on the spacetime background described in [15-17]. Fields in this background depend on the radial coordinate u ($u = 0$ at the horizon, $u = \infty$ at the boundary), which is identified with the energy scale in the dual field theory, via the UV-IR correspondence. The dilaton dependence in these solutions is indeed

$$e^{-\phi(u)} \propto \frac{1}{N} \prod_{i=1}^{\frac{r}{2}} \frac{1}{u^2\theta_i} \tag{7.12}$$

at large u.

Acknowledgements

We would like to thank S. Chakravarty for collaboration at the initial stages of this project, several useful discussions and helpful comments. We thank O. Aharony, T. Banks, M. Douglas, R. Gopakumar, D. Kutasov, H. Liu, J. Maldacena, M. Rangamani, E. Rabinovici, A. Schwimmer, E. Silverstein, W. Taylor, E. Witten and A.B. Zamolodchikov for useful discussions. S.M. would like to thank the Rutgers string group for hospitality and several stimulating discussions. The work of S.M. was supported in part by DOE grant #DE-FG02-91ER40671, and N.S. by grant #DE-FG02-90ER40542.

[2] See also [10].

Appendix A. Feynman integral for a general graph in a noncommutative theory

Here we present an expression for the Feynman integral corresponding to an arbitrary graph in a noncommutative theory, written as an integral over Schwinger parameters corresponding to each internal line. This expression reveals several generic effects of the non-commutativity, which are discussed in section 5.3. The derivation, which is somewhat technical, will not be presented here.

We begin with a scalar field theory with no derivative couplings and consider a graph G with E edges, V vertices, L loops, and external momenta p_I (the generalization to arbitrary theories is given in the next subsection). We introduce Schwinger parameters α_i for each internal line of the graph, after which the integrals over momenta may be evaluated exactly to give

$$c(g_i)\delta(\sum p^I)V(p^I)\frac{1}{2^{dL}\pi^{dL/2}}\int d\alpha_i e^{-\alpha_i m_i^2}\mathcal{I}(\alpha,\Theta,p^I). \tag{A.1}$$

Here, $c(g_i)$ is an overall constant given by the product of the symmetry factor for the graph with all vertex factors. The factor $V(p_I)$, defined in (2.6), is the overall phase, present for all graphs, which depends on the cyclic ordering of p's. The integrand $\mathcal{I}$ is

$$\mathcal{I}(\alpha,\Theta,p^I)=\frac{1}{(\prod_{\theta_a}P_G(\alpha,\theta_a))^{\frac{1}{2}}}e^{-p^I_\mu\left(\frac{S_{IJ}(\alpha,\Theta^2)}{P_G(\alpha,\Theta^2)}\right)^{\mu\nu}p^J_\nu-ip^I_\mu\left(\frac{\Theta A_{IJ}(\alpha,\Theta^2)}{P_G(\alpha,\Theta^2)}\right)^{\mu\nu}p^J_\nu}. \tag{A.2}$$

In the rest of this subsection we explain the various objects in this expression. In the denominator, the product runs over the eigenvalues θ_a of Θ. The function $P_G(\alpha,\theta)$ is a polynomial defined by

$$P_G=P(G)=\sum_{H\in R(G)}\theta^{E-V+1}\prod_{i\in H^c}\frac{\alpha_i}{\theta}. \tag{A.3}$$

Here H^c is the set of internal lines in the complement of H and $R(G)$ is the set of subgraphs H of G containing only internal lines such that H contains a maximal tree (a tree touching all vertices) of G and H has maximal genus (a single index line when drawn in double line notation)[3]. We note that P is an even polynomial in Θ, of degree $2h$, where h is the genus of the graph G (ignoring external lines).

[3] The condition of maximal genus may also be stated as $\det(C_{ij}(H/T))=1$, where C_{ij} is the intersection matrix for the single vertex graph H/T obtained by starting with H, removing external lines, and contracting all lines of T to a single point.

S and A in (A.2) are polynomial defined in terms of P as

$$\begin{aligned} S_{pq}(\alpha,\theta) &= \frac{1}{2}(P^*(G_{p=r}) + P^*(G_{q=r}) - P^*(G_{p=q})) \\ A_{pq}(\alpha,\theta) &= \frac{1}{\theta}[P^*(G_{p,q=r})P(G) - P^*(G_{p=r})P^*(G_{q=r}) \\ &\quad + \frac{1}{4}(P^*(G_{p=r}) + P^*(G_{q=r}) - P^*(G_{p=q}))^2]^{\frac{1}{2}}, \end{aligned} \tag{A.4}$$

where r is a particular external momentum (all choices give equivalent results), $G_{p=q}$ is a graph obtained by connecting external lines p and q to form a new internal line and $G_{p,q=r}$ is a graph obtained by connecting external momenta p and q to the vertex connected to r (without creating any new intersections). Here P^* means that P is to be evaluated with Schwinger parameters for any added lines set to zero.

A.1. Generalization to arbitrary theories

The result of the previous subsection may be easily generalized to arbitrary theories which may include particles of non-zero spin or derivative couplings. In terms of the momentum space Feynman integrands, these theories will have additional factors of internal and external momenta in the numerator coming from propagators or vertex factors. The resulting expressions for $\mathcal{I}$ (the Schwinger parameter integrand) may be related to the expressions obtained above for non-derivative scalar theories by the following trick.

Consider an arbitrary graph G in a general theory, and let $\{l_j\}$ be the set of internal momenta which appear (possibly more than once) in the numerator of the Feynman integral. We define a new graph G^+ as follows. For each l, let a be the vertex which l leaves. Now include two new external momenta, a momentum r^l which leaves vertex a immediately counterclockwise from l and a momentum $-r^l$ which leaves a immediately clockwise from l. Since these momenta sum to zero, they do not affect overall momentum conservation, and in fact their only effect is to multiply the integrand with an extra phase

$$e^{ir^l \times l}. \tag{A.5}$$

We may now replace all internal momenta l_μ appearing in the numerator of the Feynman integral with derivatives $-i(\Theta^{-1})_{\mu\nu}\partial_{r^l_\nu}$ acting outside the integral. The resulting integral over internal momenta is exactly the expression $\mathcal{I}(G^+)$ for the graph G^+ in a non-derivative scalar theory. Thus, if the function of momenta in the numerator of the Feynman integral for G is some polynomial $\pi(l_\mu, p_\mu)$, we have

$$\mathcal{I}_G(\alpha,\Theta) = \pi(-i(\Theta_0^{-1})_{\mu\nu}\partial_{r^l_\nu}, p_\mu)\, \mathcal{I}_{G^+}(\alpha,\Theta_0)|_{r^l_\mu=0,\Theta_0=\Theta}. \tag{A.6}$$

Here, $\mathcal{I}_{G^+}$ may be explicitly evaluated using the rules of the previous subsection for nonderivative scalar theories. In order that this expression be well defined for Θ of any rank, we must evaluate $\mathcal{I}_{G^+}$ using an invertible Θ_0 and then set $\Theta_0 = \Theta$ at the end. Interestingly, this procedure may be used to give Feynman integrals for a general theory in terms of Feynman integrals for a nonderivative scalar theory even in the commutative case of $\Theta = 0$.

References

[1] T. Filk, "Divergences in a Field Theory on Quantum Space," Phys. Lett. **B376** (1996) 53.

[2] J.C. Varilly and J.M. Gracia-Bondia, "On the ultraviolet behavior of quantum fields over noncommutative manifolds," Int. J. Mod. Phys. **A14** (1999) 1305, hep-th/9804001.

[3] M. Chaichian, A. Demichev and P. Presnajder, "Quantum Field Theory on Noncommutative Space-times and the Persistence of Ultraviolet Divergences," hep-th/9812180; "Quantum Field Theory on the Noncommutative Plane with E(q)(2) Symmetry," hep-th/9904132.

[4] M. Sheikh-Jabbari, "One Loop Renormalizability of Supersymmetric Yang-Mills Theories on Noncommutative Torus," hep-th/9903107,JHEP **06** (1999) 015.

[5] C.P.Martin, D. Sanchez-Ruiz, "The One-loop UV Divergent Structure of U(1) Yang-Mills Theory on Noncommutative R^4,"hep-th/9903077, Phys.Rev.Lett. **83** (1999) 476-479.

[6] T. Krajewski, R. Wulkenhaar, "Perturbative quantum gauge fields on the noncommutative torus," hep-th/9903187.

[7] S. Cho, R. Hinterding, J. Madore and H. Steinacker, "Finite Field Theory on Noncommutative Geometries," hep-th/9903239.

[8] E. Hawkins, "Noncommutative Regularization for the Practical Man," hep-th/9908052.

[9] D. Bigatti and L. Susskind, "Magnetic fields, branes and noncommutative geometry," hep-th/9908056.

[10] N. Ishibashi, S. Iso, H. Kawai and Y. Kitazawa, "Wilson Loops in Noncommutative Yang-Mills," hep-th/9910004.

[11] I. Chepelev and R. Roiban, "Renormalization of Quantum Field Theories on Noncommutative R^d, I. Scalars, "hep-th/9911098.

[12] H.Benaoum, "Perturbative BF-Yang-Mills theory on noncommutative R^4, "hep-th/9912036.

[13] A. Connes, M. Douglas and A. Schwarz, "Noncommutative Geometry and Matrix Theory: Compactification on Tori," hep-th/9711162, JHEP **02** (1998) 003.

[14] N. Seiberg and E.Witten, "String Theory and Noncommutative Geometry," hep-th/9908142, JHEP **09** (1999) 032.

[15] J. Maldacena and J. Russo, "Large N Limit of Non-Commutative Gauge Theories," hep-th/9908134.

[16] A. Hashimoto and N. Itzhaki, "Non-Commutative Yang-Mills and the AdS/CFT Correspondence," hep-th/9907166.

[17] S. Das, S. Kalyana Rama, S. Trivedi, "Supergravity with Self-dual B fields and Instantons in Noncommutative Gauge Theory,"hep-th/9911137.